HIPPOCAMPUS 23:1198–1211 (2013)

Chronic Over-Expression of TGFβ1 Alters Hippocampal Structure and Causes Learning Deficits

Alonso Martinez-Canabal,[1,2] Anne L. Wheeler,[1,2] Dani Sarkis,[1] Jason P. Lerch,[1,3] Wei-Yang Lu,[4] Marion S. Buckwalter,[5] Tony Wyss-Coray,[5,6] Sheena A. Josselyn,[1,2,7,8] and Paul W. Frankland[1,2,7,8]*

ABSTRACT: The cytokine transforming growth factor β1 (TGFβ1) is chronically upregulated in several neurodegenerative conditions, including Alzheimer's disease, Parkinson's disease, Creutzfeldt-Jacob disease, amyotrophic lateral sclerosis and multiple sclerosis, and following stroke. Although previous studies have shown that TGFβ1 may be neuroprotective, chronic exposure to elevated levels of this cytokine may contribute to disease pathology on its own. In order to study the effects of chronic exposure to TGFβ1 in isolation, we used transgenic mice that over-express a constitutively active porcine TGFβ1 in astrocytes. We found that TGFβ1 over-expression altered brain structure, with the most pronounced volumetric increases localized to the hippocampus. Within the dentate gyrus (DG) of the hippocampus, increases in granule cell number and astrocyte size were responsible for volumetric expansion, with the increased granule cell number primarily related to a marked reduction in death of new granule cells generated in adulthood. Finally, these cumulative changes in DG microstructure and macrostructure were associated with the age-dependent emergence of spatial learning deficits in TGFβ1 over-expressing mice. Together, our data indicate that chronic upregulation of TGFβ1 negatively impacts hippocampal structure and, even in the absence of disease, impairs hippocampus-dependent learning. © 2013 Wiley Periodicals, Inc.

KEY WORDS: hippocampus; cytokine; learning; neurodegenerative disease; dentate gyrus

[1] **Program in Neurosciences and Mental Health, Hospital for Sick Children, Toronto, Ontario, Canada;** [2] **Institute of Medical Science, University of Toronto, Toronto, Ontario, Canada;** [3] **Department of Medical Biophysics, University of Toronto, 610 University Ave., Toronto, Ontario, Canada;** [4] **Molecular Brain Research Group, Robarts Research Institute, University of Western Ontario, London, Ontario, Canada;** [5] **Department of Neurology and Neurological Sciences, Stanford University, Stanford, California;** [6] **Center for Tissue Regeneration, Repair, and Restoration, Veterans Administration Palo Alto Health Care Systems, Palo Alto, California;** [7] **Department of Physiology, University of Toronto, Toronto, Ontario, Canada;** [8] **Department of Psychology, University of Toronto, Toronto, Ontario, Canada**

Grant sponsor: Canadian Institutes of Health Research; Grant numbers: MOP86762, MOP74650; Grant sponsor: National Institutes of Health (NIH); Grant number: K08 NS050304; Grant sponsors: El Consejo Nacional de Ciencia y Tecnologia (Mexico); the Ontario Mental Health Foundation.

*Correspondence to: Paul W. Frankland, Program in Neurosciences and Mental Health, Hospital for Sick Children, Toronto, ON M5G 1X8 Canada. E-mail: paul.frankland@sickkids.ca

Accepted 4 June 2013.
DOI 10.1002/hipo.22159
Published online 5 August 2013 in Wiley Online Library (wileyonlinelibrary.com).

© *2013 WILEY PERIODICALS, INC.*

INTRODUCTION

Transforming growth factor-β1 (TGFβ1) is a widely expressed cytokine that regulates a wide range of biologic processes during development and adulthood (Massague, 2012). Within the brain it is secreted by neurons and glia, and, similar to many other cytokines it is chronically upregulated in many neurodegenerative conditions including Alzheimer's disease (Apelt and Schliebs, 2001; Zetterberg et al., 2004), amyotrophic lateral sclerosis (Hensley et al., 2003), multiple sclerosis (Link et al., 1994), Parkinson's disease (Mogi et al., 1994, 1995), prion diseases (Baker et al., 1999), and stroke (Henrich-Noack et al., 1996; Buisson et al., 2003). In these diseases, upregulation of TGFβ1 is observed within the affected brain areas, as well as cerebrospinal fluid and plasma.

TGFβ1 is neuroprotective, and therefore its upregulation in a disease state may oppose or slow neurodegeneration (Buckwalter et al., 2006; Tesseur and Wyss-Coray, 2006). For example, in mouse models, over-expression of TGFβ1 reduces cell death induced by acute or chronic neuronal insults (Brionne et al., 2003). Conversely, genetic deletion of TGFβ1 is associated with increased neurodegeneration both in vivo and in vitro (Brionne et al., 2003). Similarly, over-expression of TGFβ1 attenuates cell death during ischemia, leading to a reduction in lesion size, whereas inhibiting TGFβ1 signaling during ischemia results in a 3-fold increase in lesion size (Ruocco et al., 1999).

Although these data suggest that TGFβ1 plays a neuroprotective role in disease, opposing or slowing neurodegeneration, the long-term consequences of chronically elevated TGFβ1 levels on brain structure and function are not known. Here, we address this question using a mouse line where over-expression of a porcine TGFβ1 is driven by the astrocytic promoter, glial fibrillary acidic protein (GFAP). In these mice, there is an approximate threefold increase in overall TGFβ1 levels, an elevation that is comparable to that observed in the frontal cortex of AD patients (Wyss-Coray et al., 1995; Wyss-Coray et al., 1997). Using these mice, we found that chronic over-expression of TGFβ1 was associated with an age-dependent increase

in the size of the hippocampus. This increase was most pronounced in the DG of the hippocampus, where both neuron number and astrocyte size correlated with increased volume measured by magnetic resonance imaging. Although adult neurogenesis was reduced in the DG, a profound reduction in apoptotic cell death appeared to be responsible for increased number of dentate neurons and associated volumetric changes. These changes in DG structure were associated with an age-dependent emergence of spatial learning impairments in the water maze.

MATERIALS AND METHODS

Mice

Male and female offspring were derived from a cross between wild-type C57Bl/6 (B6) female mice (Taconic) and heterozygous male TGFβ1 mice where over-expression of a porcine TGFβ1 is driven by a GFAP promoter (Wyss-Coray et al., 1995; Wyss-Coray et al., 1997; Buckwalter et al., 2006). The TGFβ1 mice were maintained on a B6 background (>10 generations). All mice were bred in our colony at The Hospital for Sick Children, and maintained on a 12 h light/dark cycle with free access to food and water. Behavioral procedures were conducted during the light phase of the cycle by an experimenter blind to the genotype of the animals. All procedures were approved by the Animal Care Committee at The Hospital for Sick Children.

Western Blotting

Transgenic mice and their WT littermates were sacrificed and their brains were flash frozen in isopentane (Sigma) at −75°C (WT [2-month-old], $n = 4$; WT [12-month-old], $n = 4$; TGFβ1 [2 month-old], $n = 4$; TGFβ1 [12-month-old], $n = 5$). Frozen cortical and hippocampal tissues were dissected and homogenized in RIPA buffer containing 1% Nonidet P-40, 0.1% Sodium dodecyl sulphate, 0.5% Deoxycholic acid, and protease inhibitors (Sigma). Protein concentrations were assayed by the Bradford method (Bio-Rad Laboratories). Protein samples (30–60 μg) were fractionated on SDS-polyacrylamide gel electrophoresis and transferred to nitrocellulose membranes (Bio-Rad Laboratories). Membranes were blocked with 5% skim milk powder in TBS-T (0.1% Tween 20, 1 mM Tris-HCl pH 8.0 and 150 mM NaCl) (Sigma). The primary antibody used was anti-TGF-β1 (1:2,000, Cell Sciences) with HRP-conjugated Glyceraldehyde-3-phosphate dehydrogenase (GAPDH) (1:5,000, Abcam) as a loading control. The blots were incubated with a HRP-conjugated secondary antibody (goat anti-rabbit 1:10,000) and the bands detected with enhanced chemiluminescence (GE Healthcare).

Magnetic Resonance Imaging

A separate cohort of mice was used for magnetic resonance imaging (MRI) (WT [2-month-old], $n = 6$; WT [12-month-old], $n = 12$; TGFβ1 [2-month-old], $n = 6$; TGFβ1 [12-month-old], $n = 12$). Specimen preparation, imaging, and analysis were performed as described previously (Lerch et al., 2011). Briefly, mice were anaesthetized with chloral hydrate (400 mg/kg, i.p.), and perfused transcardially with phosphate buffered saline (PBS) followed by 4% paraformaldehyde (PFA) at 4°C. Bodies, along with the skin, lower jaw, ears, and the cartilaginous nose tip were removed. The remaining skull structures containing the brain were allowed to postfix in 4% PFA at 4°C for 12 h. Following a washout period of 5 days in PBS and 0.01% sodium azide at 15°C, the skulls were transferred to a PBS and 2 mM ProHance® (Bracco Diagnostics, Princeton, NJ) solution for at least 7 days at 15°C before imaging 12–21 days post-mortem.

A multichannel 7.0 T MRI scanner (Varian, Palo Alto, CA) with a 6 cm inner bore diameter insert gradient was used to acquire anatomical images of brains. Brains were imaged within skulls in order to minimize geometric distortion. Before imaging, the samples were removed from the contrast agent solution, blotted and placed into plastic tubes (13 mm in diameter) filled with a proton-free susceptibility-matching fluid (Fluorinert FC-77, 3 MCorp., St. Paul, MN). Three custom-built, solenoid coils (14 mm in diameter, 18.3 cm in length) with over wound ends were used to image three brains in parallel. Parameters used in the scans were optimized for gray/white matter contrast: a T2-weighted, 3D fast spin-echo sequence with 6 echoes, with TR/TE = 325/32 ms, four averages, field-of-view 14 × 14 × 25 mm^3, and matrix size = 432 × 432 × 780 giving an image with 32 μm isotropic voxels. Geometric distortion due to position of the three coils inside the magnet was calibrated using a precision machined MR phantom. After MRI scanning, brains were washed with PBS and stored in 10% formalin for later immunohistochemistry.

We used an image registration-based approach to assess anatomical differences related to age and genotype. Image registration finds a smooth spatial transformation that best aligns one image to another such that corresponding anatomical features are superimposed. We used an automated intensity-based group-wise registration approach (Lerch et al., 2011) to align all brains in the study into a common coordinate system, yielding an average image of the 36 MRI scans. To quantify the deformation that brought the images into alignment with the population average and provide a summary of how they differ, the Jacobian determinants of the deformation fields were then calculated as measures of volume difference at each voxel. Significant volume differences were then calculated in two ways. First, an anatomical atlas comprised of 64 distinct structures (Dorr et al., 2008) was warped onto the population average and was used to compute volumes of each structure. Second, individual voxel differences between genotypes were then calculated by comparing Jacobian determinants at each voxel. After MRI scanning, brains were washed with PBS and stored in 10% formalin for their use in NeuN and GFAP immunohistochemistry.

BrdU Administration

5-bromo-2'-deoxyuridine (BrdU; Sigma, MO) was dissolved in 0.15 M PBS and heated to 50–60°C, at a concentration of

20 mg/ml. Animals received 200 mg/kg of BrdU per i.p. injection (Kee et al., 2007a). At P60, mice either received four BrdU injections at intervals of 6 h (WT, $n = 4$; TGFβ1, $n = 4$) and were perfused 24 h later or 2 BrdU injections/day for 5 days (interval 12 h) (WT, $n = 5$; TGFβ1, $n = 6$) and were perfused 25 d later (at P85). A third group of mice received a single injection at P10 (WT, $n = 4$; TGFβ1, $n = 5$) and were perfused at P85.

Immunohistochemistry

Mice were anesthetized with chloral hydrate and perfused transcardially with PBS followed by 4% PFA. Brains were removed, fixed overnight in PFA and then transferred to 30% sucrose solution. Fifty μm coronal sections were cut using a cryostat along the entire antero-posterior extent of the hippocampus. Sections were kept in sequential order and maintained free-floating in PBS. A 1/6 section sampling fraction was used to create six sets (each containing sections at 300 μm intervals) for use in immunohistochemical staining. Accordingly, each set comprised a systematic random sample representative of the entire hippocampus for use in quantification analyses. Additional sets were stored in a PBS solution containing 50% glycerol and 10% ethylene glycol for later processing.

For BrdU staining, antigen unmasking was performed by incubating the sections in 1 N HCl at 45°C for 30 min. Sections were incubated with a primary antibody (rat anti-Brdu 1:1000, Accuarate Antibodies, N.Y) for 48 h at 4°C, and then a secondary antibody (goat anti-rat Alexa-488 1:1,000, Invitrogen, CA) for 2 h at room temperature. Antibodies were diluted in blocking solution containing 2% goat serum, 2.5% bovine serum albumin, and 0.3% Triton X-100 dissolved in PBS. Sections were mounted on slides (VWR, West Chester, PA) with Permafluor anti-fade medium (Lipshaw Immunon, Pittsburgh, PA).

For the other antigens analyzed, antigen unmasking was performed in a steamer during 40 min in a 0.01 M citrate solution with 0.01% Tween 20. They detected GFAP (mouse monoclonal 1:2,500; Cell Signaling Technology, MA) (WT [2-month-old], $n = 4$; WT [12-month-old], $n = 6$; TGFβ1 [2-month-old], $n = 6$; TGFβ1 [12-month-old], $n = 4$) NeuN (mouse monoclonal 1:1,000; Millipore, MA) (WT [2-month-old], $n = 6$; WT [12-month-old], $n = 5$; TGFβ1 [2-month-old], $n = 5$; TGFβ1 [12-month-old], $n = 5$) or Ki67 (rabbit polyclonal 1:2,500, Abcam) ([P10]: WT, $n = 5$, TGFβ1, $n = 4$; [P60]: WT, $n = 4$, TGFβ1, $n = 5$; [P150]: WT, $n = 6$, TGFβ1, $n = 5$; P360 [WT], $n = 6$, TGFβ1, $n = 4$). Signals were amplified and visualized using Vectastain Elite ABC kit (Vector Laboratories) with Diaminobenzidine (DAB) (Sigma) as a chromogen. Sections were mounted on gelatin coated slides, stained with Harris hematoxylin (Sigma) for nuclear visualization, and coverslipped using crystal mount (EM).

TUNEL staining was carried out using the DeadEnd Tunel kit® (Promega) with minor modifications to manufacturer instructions to detect apoptotic cell death in P60 mice (WT, $n = 6$, TGFβ1, $n = 7$).

Golgi-Cox Staining

Mice were perfused with PBS and whole brains were removed and impregnated with Golgi-Cox solution using the FD Rapid Golgi Stain Kit (FD neurotechnologies). After 3 weeks, coronal 120 μm sections were cut in 30% sucrose solution using a vibratome (Leica). Sections were stored in the dark, mounted on gelatin coated slides, developed with 1% NH_4OH, fixed with Kodak fixative, and then coverslipped.

Imaging

Data and images were acquired using Nikon Eclipse 80i or Olympus BX61 epifluorescent microscopes, or Zeiss LSM710 confocal microscope. Cell counting and astrocyte morphology analysis was conducted using Stereoinvestigator 9.1 (MBF Bioscience). We estimated the total number of NeuN and GFAP positive cells using the optical fractionator method on the Olympus BX61 microscope using a 60X, 1.45 N.A. objective and a motorized XYZ stage attached to a computer (Hosseini-Sharifabad and Nyengaard, 2007). Random systematic sampling was used for these stereological analyses (section interval of 1/6, grid size of 250 × 500 μm, 2D counting frame of 30 μm × 30 μm [NeuN] or 90 μm × 90 μm [GFAP] using z-axis dissectors 15 μm deep). These parameters were used to estimate the total number of cells in the entire DG, CA1 or CA3. Conditions were optimized to obtain a Gundersen coefficient of error below 0.05 (Gundersen et al., 1999). For Ki67, BrdU, and TUNEL quantifications, the total number of positive cells in a 1/6 fraction was counted, and multiplied by six times to provide an estimate of the total number of Ki67 and TUNEL positive cells. For BrdU, the average number of cells per section is reported.

Water Maze Apparatus and Procedures

The apparatus and behavioral procedures have been previously described (Teixeira et al., 2006). Behavioral testing was conducted in a circular water maze tank (120 cm in diameter, 50 cm deep), located in a dimly-lit room. The pool was filled to a depth of 40 cm with water made opaque by adding white, nontoxic paint. Water temperature was maintained at 28 ± 1°C using a heating pad beneath the pool. A circular escape platform (10 cm diameter) was submerged 0.5 cm below the water surface in a fixed position. The pool was surrounded by curtains, at least 1 m from the perimeter of the pool. The curtains were white with distinct cues painted on them.

Before training, mice were individually handled for 2 min each day over 5 consecutive days. The complete water maze training protocol consisted of three consecutive trials per day for 8 days. On each trial, the mouse was placed into the pool, facing the wall, in one of four start locations. The order of these start locations was randomly varied throughout training but similar for all animals. The trial was completed once the mouse found the platform or 60 s had elapsed. If the mouse failed to find the platform on a given trial, the experimenter guided the mouse onto the platform. At the end of each trial,

mice were allowed 15 s to rest atop the platform before beginning the next trial. Spatial memory was assessed during probe tests by removing the platform from the pool, and allowing the mouse swim for 60 s. Mice were given a probe test before training on days 1, 3, 5,7, and on day 9.

Behavioral data from training and the probe tests were acquired and analyzed using an automated tracking system (Actimetrics, IL). For the probe tests, we quantified performance in two ways. First, we measured the amount of time mice spent in the target zone (20 cm radius, centered on the location of the platform during training). This zone represents ~11% of the total pool surface. Second, we represented probe test performance as a heat map (or density plot), with hot colors corresponding to areas of the pool that were more frequently visited. During probe tests, we additionally recorded swim speed and thigmotaxis (the percentage of total time that mice swam within 5 cm of the pool walls).

Statistical Analyses

Behavioral, MRI, and cell counting data were evaluated using parametric ANOVAs or t-tests, where appropriate. Multiple comparisons were controlled for in the MRI brain volume analysis by applying the Bonferroni correction to the structure volume comparisons and the False Discovery Rate (1% FDR; (Genovese et al., 2002)) for the voxel wise whole brain comparisons.

RESULTS

Levels of TGFβ1 Over-Expression are Stable With Age

Using an anti-porcine TGFβ1 antibody we first evaluated transgenic TGFβ1 expression in 2 and 12-month-old TGFβ1 and WT littermate control mice. Analysis of homogenates from hippocampus and cortex indicated that the transgene was robustly expressed, and expression levels did not change with age (hippocampus [$t_7 = 1.40$, $P > 0.05$]; cortex [$t_7 = 1.40$, $P > 0.05$]). As expected, no transgene signal was detected in WT mice (Fig. 1).

TGFβ1 Over-Expression Produces Age-Dependent Macroscopic Changes in Brain Structure

Using high resolution, 3D magnetic resonance imaging we next evaluated the long-term consequences of TGFβ1 over-expression on brain structure. Brains from young (2 month-old) and old (12-month-old) control and TGFβ1 mice were scanned and digitized using a multichannel 7.0 Tesla MRI scanner (Fig. 2a). Unbiased, computer-generated atlases were then created for all MR scans, which were then deformed into exact alignment with one another. Subsequent quantitative volume differences of individual mouse neuroanatomical features

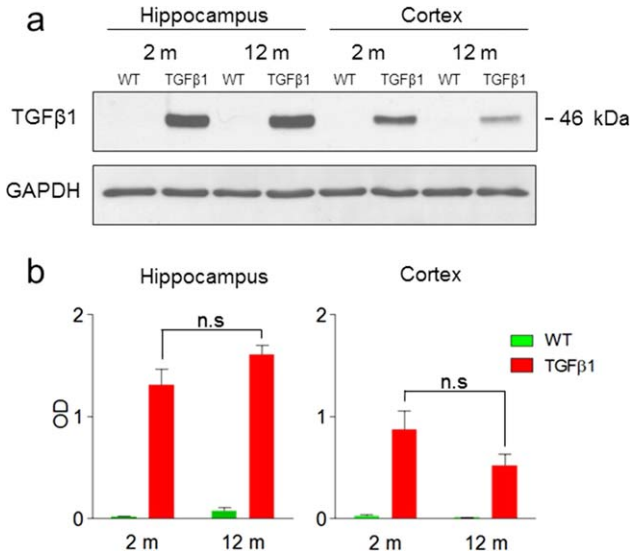

FIGURE 1. Expression of porcine TGFβ1 in hippocampus and cortex. a. Representative western blot of TGFβ1 precursor peptide (46 kDa) in hippocampal and cortical tissue from young (2 month-old) and aged (12-month old) TGFβ1 mice and their WT littermates. b. Ratio of optical densities (OD) of TGFβ1 vs. GAPDH (loading control) bands for TGFβ1 mice and their WT littermates. Levels of TGFβ1 did not change with age in hippocampus or cortex. [Color figure can be viewed in the online issue, which is available at wileyonlinelibrary.com.]

were determined using a composite brain atlas (Dorr et al., 2008). In aged, 12-month-old TGFβ1 mice, these analyses confirmed that TGFβ1 over-expression was associated with enlargement of the 3rd and lateral ventricles, as previously reported (Wyss-Coray et al., 1995). In addition to hydrocephalus, total brain volume was increased in TGFβ1 mice at both ages (genotype main effect: $F_{1,31} = 29.82$, $P < 0.01$) (Fig. 2b). The volume of many forebrain, midbrain, and hindbrain regions was increased, and the most pronounced changes were observed in hippocampal CA3 and DG (both granule cell and molecular layers) regions (Fig. 2c). In contrast, similar volumetric changes were not observed in young, 2-month-old TGFβ1 mice.

TGFβ1 Over-Expression is Associated with Age-Dependent Increases in Astrocyte Size in DG

The MRI analyses revealed that chronic over-expression of TGFβ1 mice led to age-dependent, macroscopic changes in brain structure. These were especially pronounced in the hippocampus, and, in particular, the molecular and granule cell layers of the DG. As the molecular layer is predominantly composed of astrocytes, and previous studies have shown that TGFβ1 activates astroglia, leading to increased branching and soma size (de Sampaio e Spohr et al., 2002; Reilly et al., 1998; Sousa Vde et al., 2004), we next asked whether changes in astrocyte number and/or morphology could account for increased molecular layer volume in aged, TGFβ1 mice. To do this we cut sections from the same MRI-scanned brains and

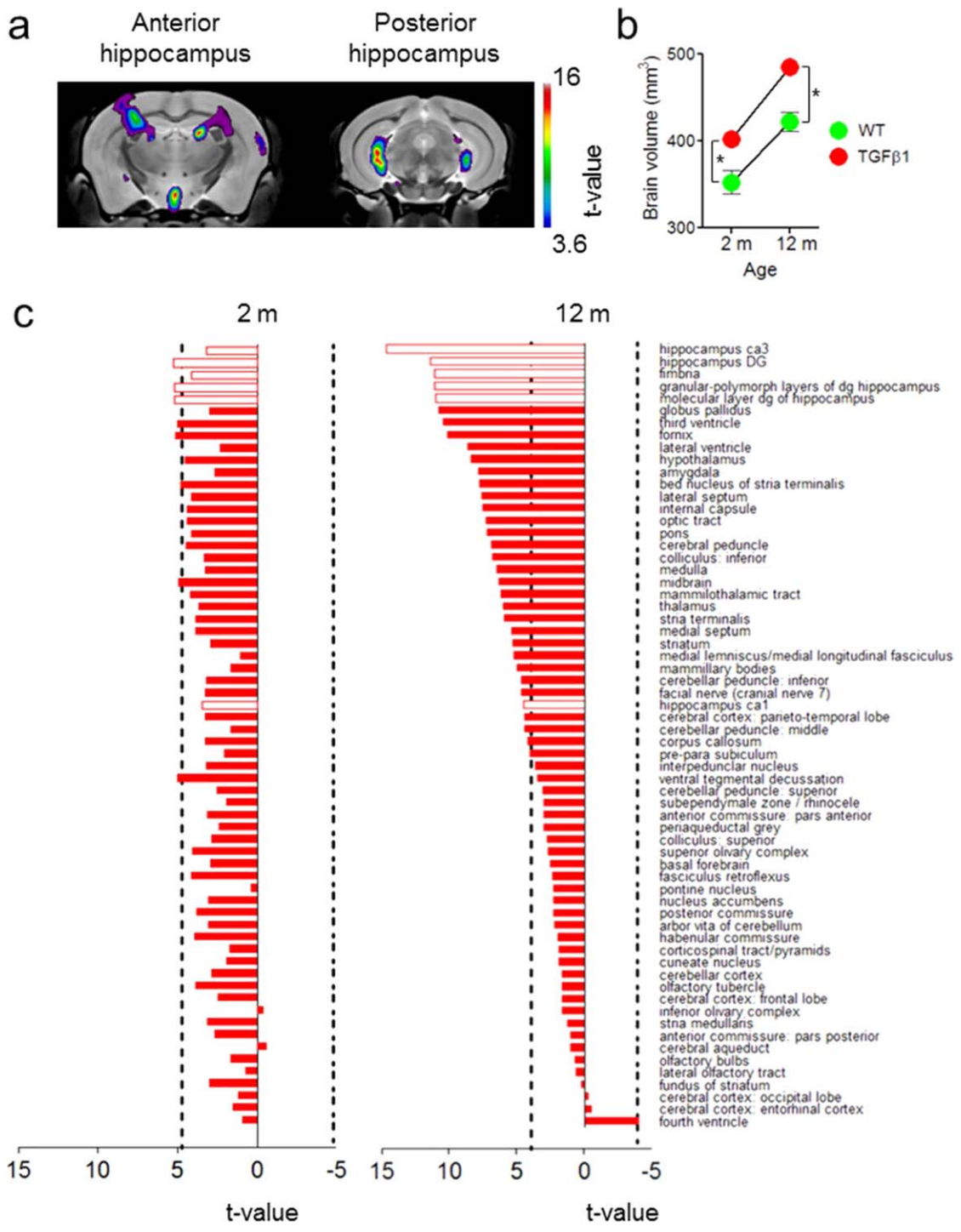

FIGURE 2. Volumetric changes in brain structure measured with MRI following TGFβ1 over-expression. a. Coronal view of voxel wise increases in volume in aged TGFβ1 mice localized to the anterior and posterior hippocampi (1% FDR). The color scale indicates the significance of the difference by Student-t value. b. The volume of the whole brain is larger in TGFβ1 mice. c. The effect size of volumetric changes both in young (left) and aged (right) TGFβ1 mice are shown for each of the 64 brain structures (hippocampal structures; open bars). The effect size is shown by Student-t values where the critical value for $P < 0.05$ is shown after Bonferroni correction (lines). Volume was increased in hippocampal CA3, granule cell layer of the DG and molecular cell layer of the DG in aged TGFβ1 mice. Thirty six structures in the aged group of animals are larger than those of their WT littermates. Nine of those structures are also larger in the young transgenic mice, including the subdivisions of the DG. [Color figure can be viewed in the online issue, which is available at wileyonlinelibrary.com.]

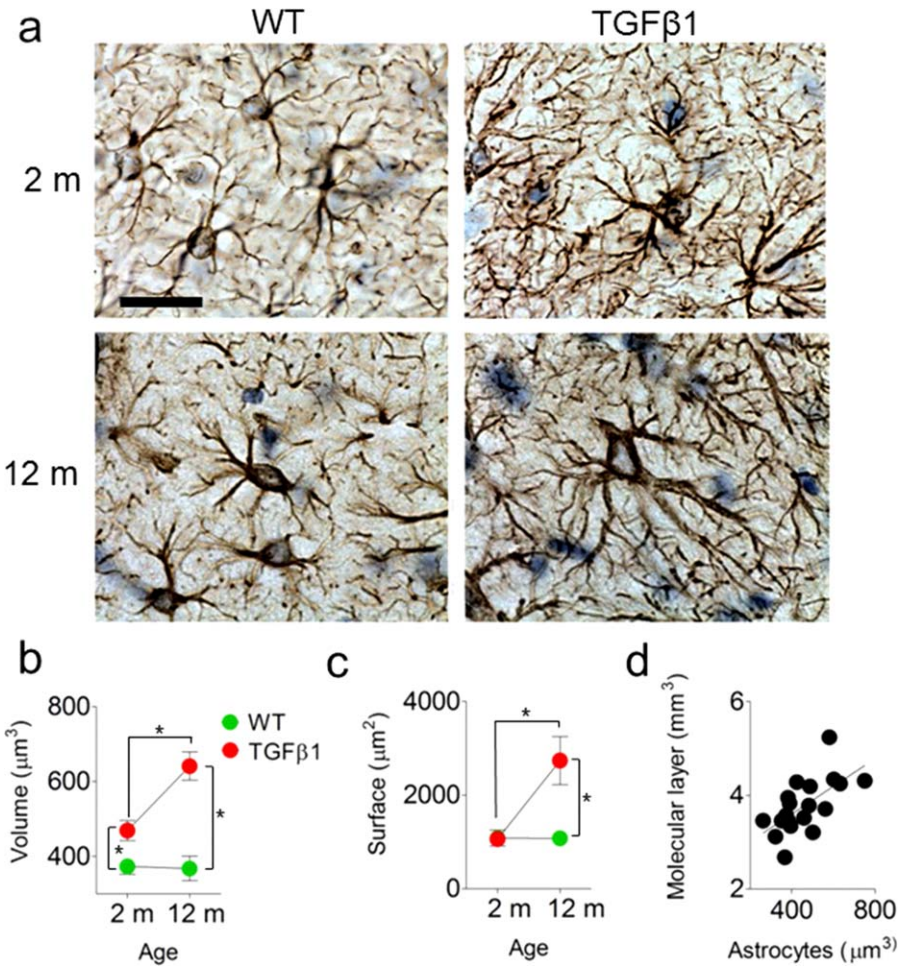

FIGURE 3. Age-dependent changes in astrocyte morphology following TGFβ1 over-expression. a. Representative images of astrocytes in the DG in young (2 m) and aged (12 m) WT and TGFβ1 mice. Scale bar = 20 μm. b. Astrocytes were enlarged in TGFβ1 mice compared to WT littermate controls. c. Surface area was increased in aged TGFβ1 mice. d. MRI-measured molecular layer volume correlated with immunohistochemical estimates of astrocyte volume in young and old TGFβ1 mice. [Color figure can be viewed in the online issue, which is available at wileyonlinelibrary.com.]

stained for the astrocytic marker GFAP (Fig. 3a). Although overall numbers of astrocytes did not vary with age or genotype (no significant genotype or age × genotype interactions; data not shown), we observed age-dependent changes in astrocyte size in TGFβ1 mice. Both astrocyte volume (significant age × genotype interaction: $F_{1,16} = 7.90$, $P < 0.05$; Fig. 3b) and total surface area (significant age × genotype interaction: $F_{1,16} = 11.92$, $P < 0.01$; Fig. 3c) were increased in aged, TGFβ1 mice, suggesting that age-dependent astrocytic growth may account for increased molecular layer volume in TGFβ1 mice. Consistent with this, within animals there was a high degree of correspondence between MRI-measured molecular layer volume and immunohistochemistry-based estimates of astrocyte volume (Regression analysis for MRI- and immunohistochemistry-based measures for all four groups: Pearson's $r = 0.65$, $P < 0.005$) (Fig. 3d). This within-animal correspondence suggests that changes in astrocyte size contribute significantly to increased molecular layer volume in TGFβ1 mice.

TGFβ1 Over-Expression is Associated with Age-Dependent Increases in Neuron Number in DG

The MRI analyses also revealed age-dependent increases in the volume of the dentate granule cell layer in aged, TGFβ1 mice. As the granule layer is almost exclusively composed of neurons (and very few astrocytes), this raises the possibility that chronic over-expression of TGFβ1 leads to a net increase in the number of dentate granule cells. To address this we cut sections from the same MRI-scanned brains and stained for the mature, neuronal marker NeuN. Stereological quantification revealed age-dependent increases in numbers of $NeuN^+$ cells in TGFβ1 mice in the dentate granule cell layer (significant age × genotype interaction: $F_{1,16} = 18.31$, $P < 0.001$): Whereas in young WT and TGFβ1 mice there were similar numbers of $NeuN^+$ cells, in aged mice, there were roughly 1.4 fold more $NeuN^+$ cells in TGFβ1 mice (Fig. 4a). In contrast, we found no evidence for increased neuron number in non-neurogenic

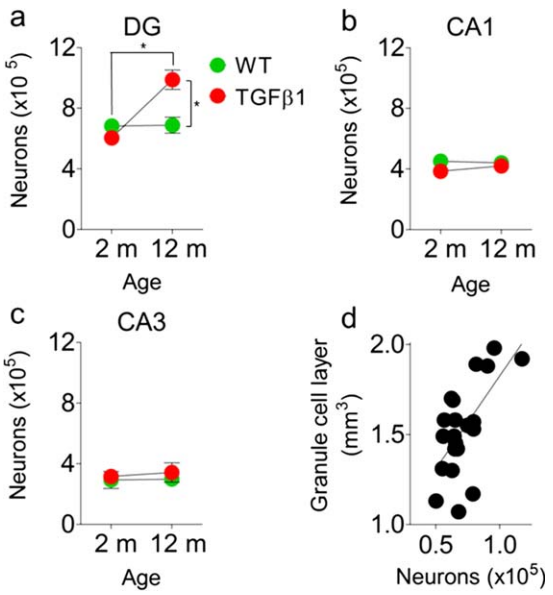

FIGURE 4. Age-dependent changes in granule cell number following TGFβ1 over-expression. Neurons in in young (2 m) and old (12 m) WT and TGFβ1 mice in (a) DG, (b) CA1 and (c) CA3. d. MRI-measured granule cell layer volume correlated with immunohistochemical estimates of granule cell number in young and old TGFβ1 mice. [Color figure can be viewed in the online issue, which is available at wileyonlinelibrary.com.]

CA1 and CA3 regions of the hippocampus (no significant genotype or age × genotype interactions; Fig. 4b,c). These findings suggest the possibility that a net increase in the number of dentate granule cells accounts for the observed, MRI-measured increase in dentate granule cell layer volume. To directly examine this, we next asked to what extent do MRI-measured granule cell layer volume and immunohistochemistry-based estimates of neuron number correspond across mice. Similar to the analysis of astrocytes in the molecular layer, we found that within animals there was a high degree of correspondence between MRI-measured granule cell layer volume and immunohistochemistry-based estimates of neuron number (Regression analysis for MRI- and immunohistochemistry-based measures for all 4 groups: Pearson's $r = 0.64$, $P < 0.01$) (Fig. 4d). This within-animal correspondence suggests that a net increase in neuron number accounts, in part, for increased dentate granule cell layer volume in aged, TGFβ1 mice. We additionally found a within animal correspondence between MRI-measured CA3 volume and immunohistochemistry-based estimates of granule cell number in the DG (Regression analysis for MRI- and immunohistochemistry-based measures for all four groups: Pearson's $r = 0.55$, $P < 0.01$, data not shown). This observation suggests that an expansion of the mossy fiber projection may also contribute to volumetric expansion of CA3 in TGFβ1 mice.

Increased Neuron Number is Associated With Altered Granule Cell Morphology and Dentate Neuroanatomy

Our experiments indicate that TGFβ1 over-expression led to an increase in the number of dentate granule cells. We next asked whether this increase in neuron number altered overall DG neuroanatomy and dentate granule cell morphology in TGFβ1 mice. To examine gross DG neuroanatomy, we inspected nissl-stained sections through the anterior–posterior extent of the hippocampus. Strikingly, we found a consistent, age-dependent change in the shape of DG granule cell layer (Fig. 5a). In normal mice, the DG comprises an upper and lower blade, joined by a single, acute fold. In contrast, in aged TGFβ1 mice there were typically additional folds in the upper blade. To quantify this we measured the "caliper" distance (van der Worp et al., 2001) between the upper and lower blades in TGFβ1 and littermate control mice. Consistent with additional folds in the upper blade, we found that TGFβ1 over-expression increased the interblade distance, and this was more pronounced in aged, TGFβ1 mice (significant age × genotype interaction: $F_{1,97} = 4.09$, $P < 0.05$) (Fig. 5b).

To examine the morphology of dentate granule cells, we next impregnated a separate set of brains using the Golgi-Cox method and several indices of dendritic complexity were computed in TGFβ1 compared with WT mice. At both ages we found that TGFβ1 over-expression reduced dendritic complexity of granule cells (Fig. 5c). Sholl analysis revealed that there was a reduction in total dendritic length in both young ($F_{1,52} = 34.54$, $P < 0.001$) and aged TGFβ1 mice ($F_{1,60} = 6.58$, $P < 0.05$) (Fig. 5d,e). Consistent with this there was a reduction in total number of intersections in both young ($F_{1,51} = 10.99$, $P < 0.01$) and aged TGFβ1 mice ($F_{1,60} = 11.52$, $P < 0.01$) (Fig. 5f,g). An identical pattern of results was found using alternate measures of complexity, such as density of bifurcation nodes (data not shown). In addition to reduced complexity, granule cells in TGFβ1 mice had less expansive dendritic arbors (Fig. 5h). This reduction was most pronounced in aged TGFβ1 mice (significant age × genotype interaction: $F_{1,16} = 7.90$, $P < 0.05$; Fig. 5i). Together, these analyses reveal that TGFβ1 over-expression is associated with age-dependent changes in the microstructure as well as the macrostructure of the DG. In particular, increased granule cell layer folding and reduced granule cell complexity may represent consequences of neuronal over-population of the granule cell layer.

Increased Neuron Number is Associated With Reduced Apoptotic Cell Death in the DG

Our analyses reveal that TGFβ1 over-expression leads to age-dependent increases in neuron number in the DG. As the DG is one of two brain regions where neurogenesis persists throughout life (Zhao et al., 2008), this raises the possibility that hippocampal neurogenesis is altered in these mice. Consistent with this, previous studies have shown that TGFβ1 modulates adult neurogenesis in the hippocampus (Buckwalter et al., 2006). However, paradoxically, TGFβ1 over-expression resulted in a reduction, rather than increase, in proliferation (Buckwalter et al., 2006). An alternative possibility is that TGFβ1 over-expression reduces death of newborn cells, and therefore, compensates for reduced levels adult neurogenesis.

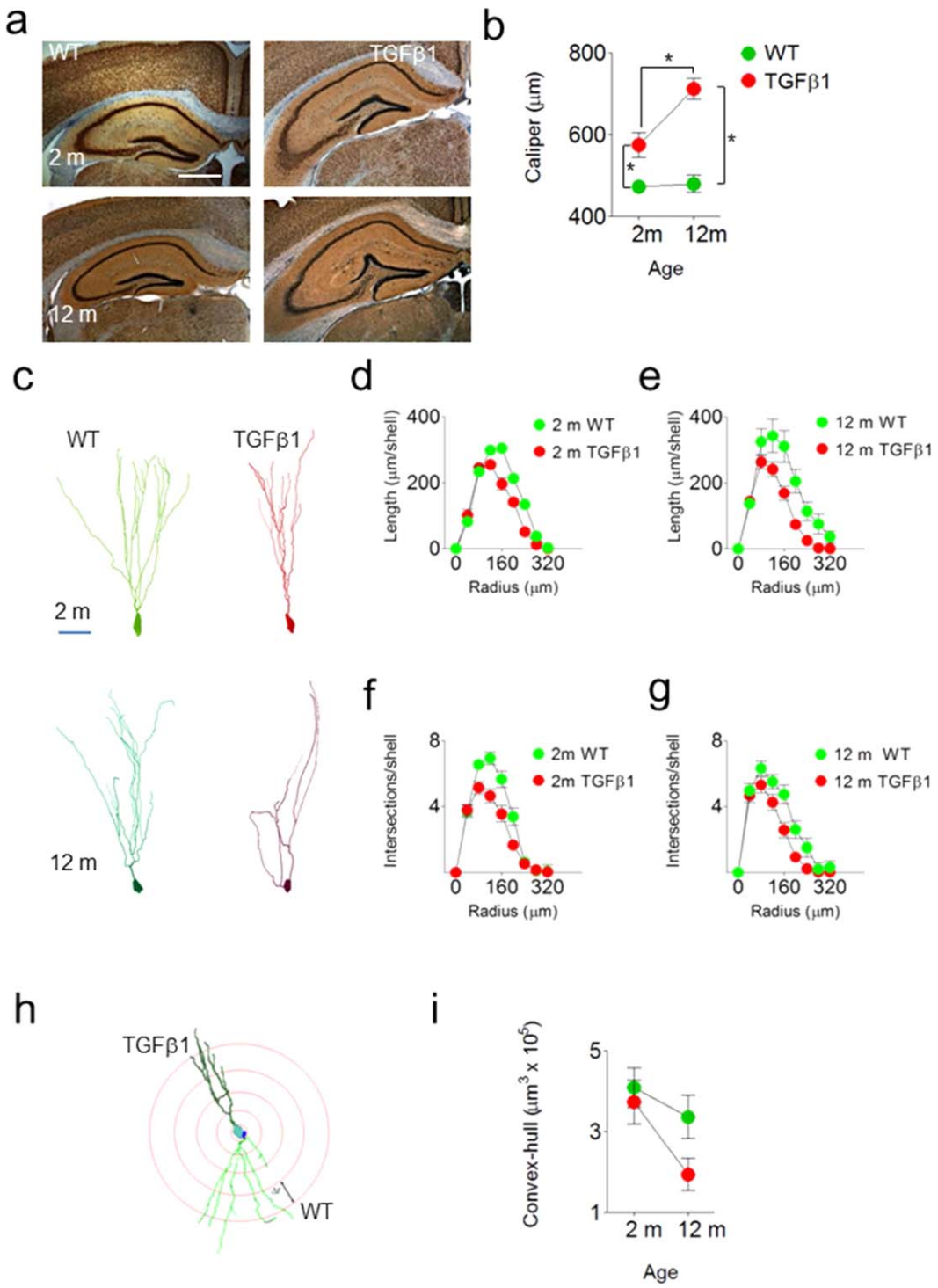

FIGURE 5. Altered DG anatomy following TGFβ1 overexpression. a. Abnormal blade folding in aged TGFβ1 mice. In normal mice, the DG comprises an upper and lower blade, joined by a single, acute fold. In contrast, there were typically additional folds in the upper blade in aged TGFβ1 mice. Scale bar = 100 μm. b. The caliper distance between the upper and lower blades is increased in young (2 m) and aged (12 m) TGFβ1 mice. c. representative Golgi-Cox impregnated granule cells in young (2 m) and aged (12 m) WT and TGFβ1 mice. Scale bar = 20 μm. Sholl analysis indicates that total dendritic length (d-e) and number of intersections (f-g) were reduced in young and aged TGFβ1 mice. h. Representative reconstructions of granule cells illustrating less expansive dendritic arbor in aged TGFβ1 mice. i. Quantification of reduced less expansive dendritic arbor in in aged TGFβ1 mice using Convex-hull method. [Color figure can be viewed in the online issue, which is available at wileyonlinelibrary.com.]

Consistent with this, in neuronal cultures exogenous application TGFβ1 is neuroprotective (Buisson et al., 1998; Dhandapani et al., 2003; Ruocco et al., 1999), and similar effects have been observed in vivo (Brionne et al., 2003).

To address these questions, we first examined levels of proliferation in the dentate by quantifying expression of Ki67 in the DG (Fig. 6a,b). Ki67 is a cell cycle related nuclear protein, expressed by proliferating cells in all phases of the active cell cycle (Kee et al., 2002). At P10, Ki67 expression was equivalent in WT and TGFβ1 mice ($t_8 = 0.32$, $P > 0.05$), suggesting that postnatal neurogenesis is unaffected by TGFβ1 over-expression. At P60 (or 2 months), Ki67 expression was reduced in TGFβ1 mice ($t_7 = 3.28$, $P < 0.05$), and this reduction was even more pronounced at later time-points (5 months [$t_9 = 5.21$, $P < 0.001$], 12 months [$t_8 = 3.43$, $P < 0.01$]). Therefore, consistent with previous reports (Buckwalter et al., 2006), these data indicate that chronic over-expression of TGFβ1 leads to reduced neurogenesis in adulthood.

Next, to evaluate whether apoptotic cell death in the DG is reduced in adult, TGFβ1 mice we stained for TUNEL, a marker of programmed cell death (Fig. 6c). Strikingly, TUNEL staining was reduced by approximately fourfold in 2-month-old TGFβ1 mice ($t_{11} = 3.19$, $P < 0.001$), suggesting that apoptotic cell death is reduced by TGFβ1 over-expression (Fig. 6d). As TUNEL staining in both WT and TGFβ1 mice was largely limited to the subgranular zone, the neuroproliferative region of the DG, this suggests that fewer newborn cells are dying in adult TGFβ1 mice. Consistent with this conclusion, no $TUNEL^+$ cells were detected in the DG in 12 month-old WT and TGFβ1 mice (data not shown), when neurogenesis levels are greatly reduced.

To more directly address whether fewer newborn cells are dying in adult TGFβ1 mice we next injected 2 month-old WT and TGFβ1 mice with the proliferation marker BrdU and waited either 1 or 45 days. Consistent with our Ki67 data, there was an approximate 50% reduction in BrdU labeling in TGFβ1 mice at the 1 d survival delay ($t_6 = 5.63$, $P < 0.01$) (Fig. 6e), indicating that adult neurogenesis is reduced. However, after 45 d equivalent numbers of BrdU-labeled cells were found in WT and TGFβ1 mice ($t_9 = 0.50$, $P > 0.05$) (Fig. 6f). Consistent with the TUNEL data, these results suggest that a reduction in cell death masks a reduction in levels of proliferation in adulthood. In contrast, there was no difference in the long-term survival rates of cells generated postnatally (at P10; $t_7 = 0.38$, $P > 0.05$) (Fig. 6g).

TGFβ1 Over-Expression is Associated With Age-Dependent Deficits in Spatial Learning

Our experiments indicate that TGFβ1 over-expression produced age-dependent changes in brain anatomy both at the macroscale (i.e., brain region) and microscale (e.g., neuronal and astocytic morphology) levels. These changes were especially pronounced in the hippocampus, a region that plays an important role in learning and memory, and is impacted in memory disorders including Alzheimer's disease (Cook, 1979). Therefore, to evaluate whether these changes in structure impacted hippocampal function, we trained both young (2-month-old) and old (12 month-old) WT control and TGFβ1 mice in the water maze. We chose a hidden version of the task where both spatial memory acquisition and expression depend on the hippocampus (Teixeira et al., 2006). Mice were trained with three trials per day for 8 days (Fig. 7a). While escape latencies declined in all groups during training (significant main effect of training: $F_{5,553} = 31.95$, $P < 0.001$), latencies were longer in aged, TGFβ1 mice (significant age × genotype interaction: $F_{1,79} = 7.05$, $P < 0.01$), suggesting that chronic over-expression of TGFβ1 impairs spatial learning (Fig. 7b).

Throughout the course of training, spatial bias was additionally assessed with a series of probe tests. In three groups (young WT, young TGFβ1 and aged WT), the selectivity of searching in these probe tests increased over time: Mice in these groups spent more time searching the target vs. other zone in the probe tests on days 5, 7, and 9 (planned comparisons for time spent in target vs. other; all Ps < 0.05). In contrast, aged TGFβ1 mice did not search selectively in the target zone in any of the probe tests (planned comparisons for probe tests on days 1, 3, 5, 7, and 9 contrasting time spent in target vs. other; all Ps > 0.05) (Fig. 7c). An ANOVA examining time spent in target zone with age and genotype as between subject variables revealed a significant age × genotype × day interaction ($F_{1,79} = 6.87$, $P < 0.05$) (Fig. 7d), confirming that chronic over-expression of TGFβ1 leads to spatial learning deficits in aged mice. A similar pattern of results was obtained using alternate metrics of water maze probe test performance (data not shown). These age-dependent deficits in TGFβ1 mice were not due to nonspecific effects on motor function, as swim speed in the probe tests was equivalent in all groups (no main effects of age, genotype or significant age × genotype interaction; Fig. 7e). Additionally, age-dependent deficits in TGFβ1 do not appear to be associated with an increased prevalence of non-spatial search strategies. At the beginning of training, naïve mice tend to spend more time searching near the walls of the pool. Whereas we found that thigmotaxic behavior was more prevalent in aged vs. young groups (significant main effect of age: $F_{1,79} = 11.57$, $P < 0.05$), it was not selectively affected in aged, TGFβ1 mice (no significant age × genotype or significant age × genotype × day interactions; Fig. 7f). Together, these data indicate that chronic over-expression leads to age-dependent deficits in spatial learning.

DISCUSSION

Under nonpathological conditions, TGFβ1 expression is relatively scarce (Lindholm et al., 1992; Nichols and Finch, 1991). However, it is rapidly and transiently upregulated in response to brain injury, and is chronically upregulated in many degenerative conditions including Alzheimer's disease, Parkinson's disease, amyotrophic lateral sclerosis, multiple

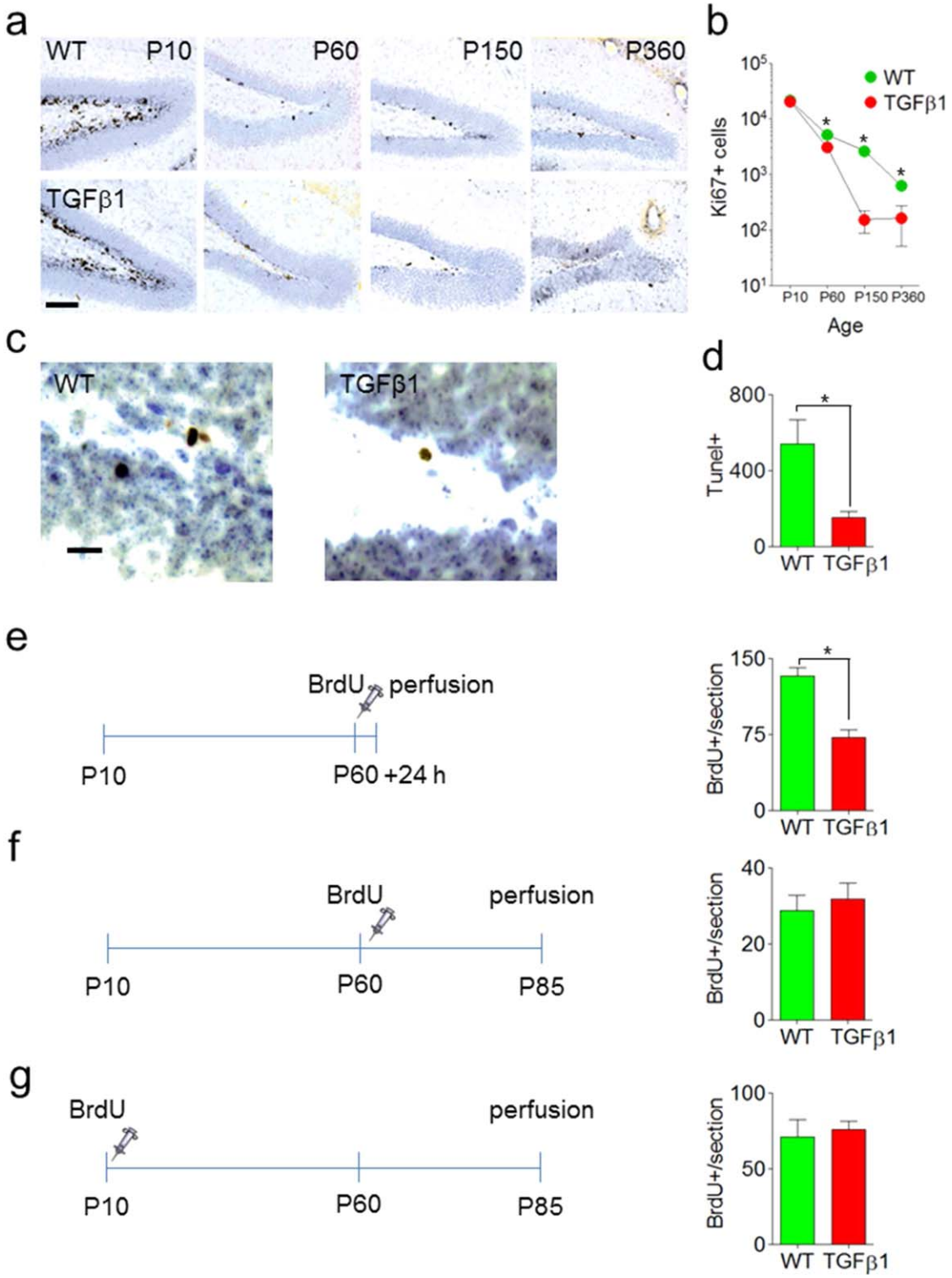

FIGURE 6. Reduced adult neurogenesis and reduced apoptotic cell death following TGFβ1 over-expression. a. Representative sections stained for proliferation marker Ki67 in DG in P10–360 WT and TGFβ1 mice. Scale bar = 50 μm. b. Number of Ki67$^+$ cells is reduced in TGFβ1 mice from P60 on, reflecting reduced proliferation in DG. Note that scale is logarithmic. c. Representative images of TUNEL$^+$ cells in DG WT and TGFβ1 mice at P60. Scale bar = 20 μm. d. TUNEL$^+$ cells were reduced approximately fourfold in TGFβ1 mice. For example, experimental scheme for BrdU injections (left) and resulting numbers of BrdU$^+$ cells in DG in WT and TGFβ1 mice (right). [Color figure can be viewed in the online issue, which is available at wileyonlinelibrary.com.]

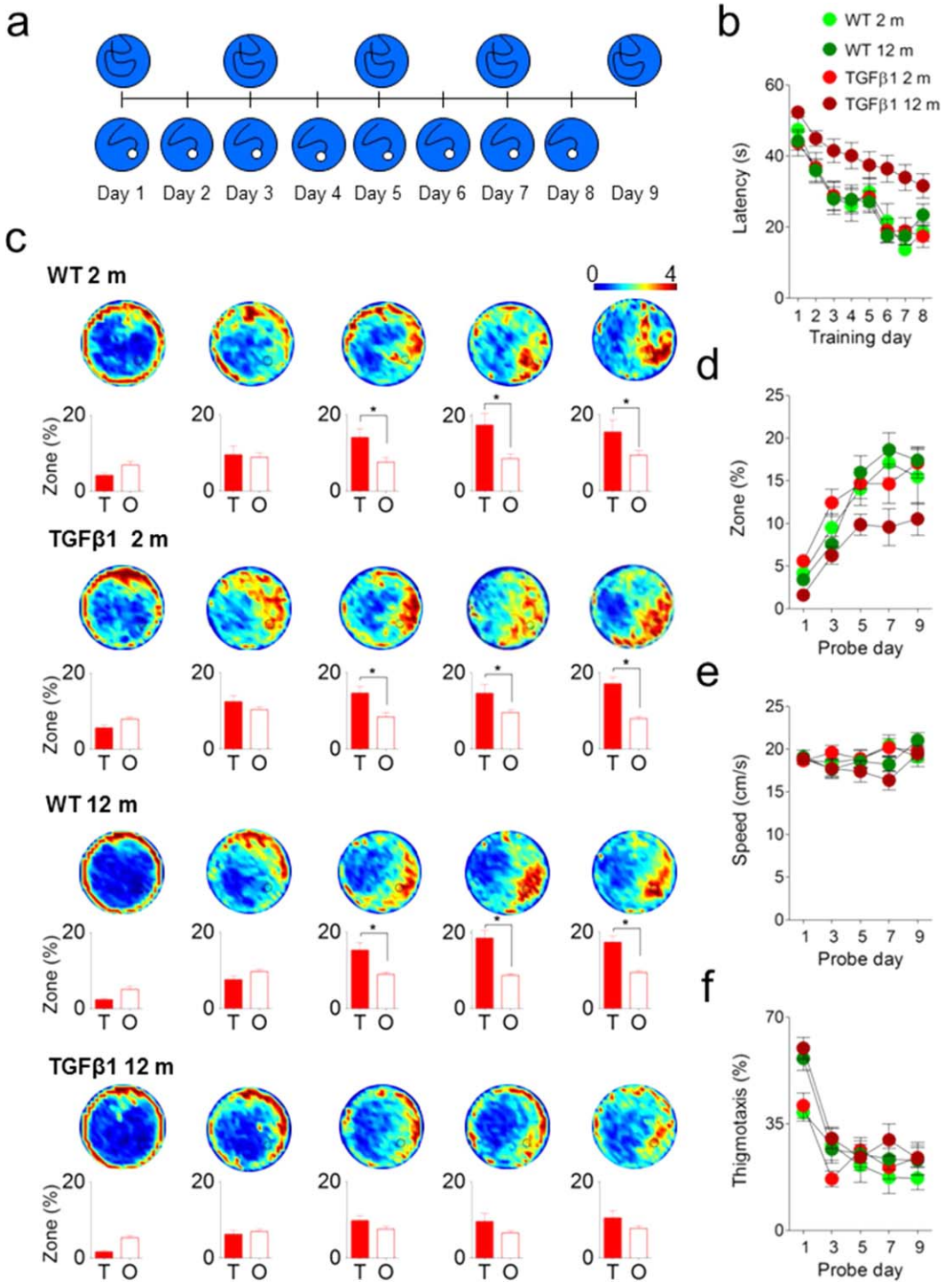

FIGURE 7. Emergence of spatial learning deficits in TGFβ1 mice. a. Experimental design for water maze. b. Latency to reach escape platform in young (2 m) and aged (12 m) WT and TGFβ1 mice during training. c. Density plots showing where mice concentrated their search for the platform during the probe tests on days 1, 3, 5, 7, and 9, with color scale representing average number of visits per mouse per 5 × 5 cm^2 area (upper). Shown below density plots are quantified data for time spent searching target (T) zone vs. other (O) zones in each of the probe tests. Chance searching is ~ 11%. d-f. During probe tests, (d) time spent in target zone, (e) swim speed, and (f) thigmotaxic behavior for young and aged WT and TGFβ1 mice. [Color figure can be viewed in the online issue, which is available at wileyonlinelibrary.com.]

sclerosis, and prion diseases such as Creutzfeldt-Jakob disease (Pratt and McPherson, 1997). To evaluate how chronic up-regulation of TGFβ1 impacts brain structure and function, we examined young (2-month-old) and aged (12-month-old) transgenic mice over-expressing a constitutively activated porcine TGFβ1 in astrocytes. Our MRI analyses revealed changes

in the volume of many brain regions, including the hippocampus. These changes were particularly pronounced in the DG, with increases in granule cell number and astrocyte size in the granule cell and molecular layers, respectively, accounting for increased DG volume. While adult neurogenesis was roughly halved in the DG, there was an approximate fourfold reduction in apoptotic cell death, consistent with the neuroprotective role of TGFβ1, as well as age-dependent increases in granule cell number. Finally, these microscopic and macroscopic level changes in DG structure were associated with deficient hippocampus-dependent learning in the water maze.

We used high resolution MRI to systematically track global changes in brain structure. Our analyses indicated that chronic upregulation of TGFβ1 alone led to profound changes in brain structure. There was an overall increase in brain volume, an increase that is driven in part by ventricular enlargement (or hydrocephalus) as has been previously reported in TGFβ1 over-expressing mice (Wyss-Coray et al., 1995). However, we additionally identified volumetric increases in a number of forebrain structures. These included the parietal cortex, medial and lateral septum, amygdala, and the mammillary bodies many of which represent brain regions that play central roles in memory and cognition (Aggleton and Brown, 2006). However, the most pronounced volumetric changes were localized to the hippocampus, and in particular the DG. Within the DG, histological analyses revealed increased neuron number in the granule cell layer and astrocyte size. These changes in microstructure following TGFβ1 over-expression appeared to be partly responsible for changes in macrostructure since variation in neuron number and astrocyte size accounted for ~45% and 41% of the variance of MRI-measured dentate volume, respectively. Furthermore, dentate granule cells had less dendritic complexity, and, in particular, had less expansive arborization. This latter phenotype might reflect neuronal "overcrowding" in aged, TGFβ1 over-expressing mice.

The DG is one of two regions in the adult brain where neurogenesis persists into adulthood (Zhao et al., 2008). While there was a net increase in total granule cells in the DG in TGFβ1 over-expressing mice, paradoxically we found that levels of adult neurogenesis were reduced by roughly half (see also (Buckwalter et al., 2006)). Instead, it appears that a reduction in apoptotic cell death of newly generated dentate granule cells is responsible for the net increase in neurons number in TGFβ1 over-expressing mice as we found a roughly fourfold reduction in TUNEL-positive cells in the DG. As these $TUNEL^+$ cells were localized to the SGZ, this suggests that TGFβ1 over-expression leads to an increase in granule cell number by selectively inhibiting apoptotic cell death of newly generated cells. There are a number of different mechanisms by which this may occur. For example, the neuroprotective effects of TGFβ1 may be mediated by upregulation of the type I plasminogen activator inhibitor (PAI-1) in astrocytes (Buisson et al., 1998; Docagne et al., 1999). Previous studies have shown that in response to increased TGFβ1 levels, astrocytes secrete PAI-1, which inhibits NMDA-mediated excitotoxicity. An alternative possibility is that increased TGFβ1 levels reduce apoptotic cell death via activation of anti-apoptotic ERK/BAD signaling in neurons (Nunez and del Peso, 1998; Zhu et al., 2001; Zhu et al., 2002). Regardless of the precise mechanism, interestingly an absence of cell loss in the DG is also observed in AD (West et al., 1994; West et al., 2004). Therefore, this raises the possibility that the absence of granule cell loss in the DG in AD patients is in part due to elevated TGFβ1 levels.

The hippocampus, including the DG, regulates memory formation (Eichenbaum, 2004). Consistent with the microscale and macroscale alterations in dentate architecture we found that TGFβ1 over-expressing mice had impaired spatial learning in a hippocampus-dependent version of the water maze, where mice were trained to locate a hidden platform in a fixed location. Like some (but not all) of the structural alterations, impairments in this spatial learning task emerged in an age-dependent manner: Relative to WT littermate controls, only aged (12-month-old), and not young (2-month-old) TGFβ1 over-expressing mice were slower in locating the platform during training and in developing a spatial bias for the trained platform location in probe tests. The delayed emergence of these deficits suggests that the impact of TGFβ1 overexpression is cumulative.

A number of circuit- and cellular-level alterations might contribute to the observed learning deficits in TGFβ1 mice. First, the relative quiescence of dentate granule cells ensures that the DG relays a sparse code onto target cells in the CA3, and this sparsification is thought to be critical for memory formation and, especially, pattern separation (Treves and Rolls, 1994; Treves et al., 2008). Increasing the number of dentate granule cells may therefore compromise sparsification and the ability of DG-CA3 to pattern separate. Second, cell death in the DG appears be necessary for normal dentate function, and therefore, reduced cell death in TGFβ1 over-expressing mice may contribute to impairments in hippocampal dependent learning. For example, pharmacological or genetic inhibition of cell death in the DG impairs spatial learning (Dupret et al., 2007; Kim et al., 2009; Lee et al., 2012). Third, as attenuated cell death is coupled with a reduction in adult neurogenesis, neuronal turnover in the dentate is greatly attenuated in TGFβ1 over-expressing mice. Recent models have proposed that the turnover of neurons in the DG may play an important role in memory regulation (Meltzer et al., 2005; Inokuchi, 2011), and therefore, reduced turnover in TGFβ1 over-expressing mice may contribute to impairments in hippocampal dependent learning. Fourth, TGFβ signaling pathways modulate synaptic plasticity in the adult brain (Krieglstein et al., 2011), including in particular the maintenance of persistent late-phase LTP in CA1 (Ageta et al., 2010). Therefore, dysregulation of hippocampal TGFβ1 levels may impair synaptic plasticity required for the formation of spatial memories. As learning deficits in TGFβ1 mice emerged with age, this may suggest that circuit level disruptions associated with TGFβ1 overexpression (which would gradually accumulate with age) rather than cellular level changes associated with TGFβ1 overexpression (which would always be present) contribute most profoundly to the spatial learning deficits.

CONCLUSIONS

Here, we examined the impact of chronic upregulation TGFβ1 in the absence of disease. Our analyses identified macroscale and microscale changes in hippocampal structure, and associated with this, deficits in hippocampal dependent learning. Together these structure-function changes suggest that while TGFβ1 may be neuroprotective, chronic upregulation may contribute to disease pathology itself.

REFERENCES

Ageta H, Ikegami S, Miura M, Masuda M, Migishima R, Hino T, Takashima N, Murayama A, Sugino H, Setou M, Kida S, Yokoyama M, Hasegawa Y, Tsuchida K, Aosaki T, Inokuchi K. (2010). Activin plays a key role in the maintenance of long-term memory and late-LTP. Learn Mem 17:176–185.

Aggleton JP, Brown MW. (2006). Interleaving brain systems for episodic and recognition memory. Trends Cogn Sci 10:455–463.

Apelt J, Schliebs R. (2001). Beta-amyloid-induced glial expression of both pro- and anti-inflammatory cytokines in cerebral cortex of aged transgenic Tg2576 mice with Alzheimer plaque pathology. Brain Res 894 21–30.

Baker CA, Lu ZY, Zaitsev I, Manuelidis L. (1999). Microglial activation varies in different models of Creutzfeldt-Jakob disease. J Virol 73:5089–5097.

Brionne TC, Tesseur I, Masliah E, Wyss-Coray T. (2003). Loss of TGF-beta 1 leads to increased neuronal cell death and microgliosis in mouse brain. Neuron 40:1133–1145.

Buckwalter MS, Yamane M, Coleman BS, Ormerod BK, Chin JT, Palmer T, Wyss-Coray T. (2006). Chronically increased transforming growth factor-beta1 strongly inhibits hippocampal neurogenesis in aged mice. Am J Pathol 169:154–164.

Buisson A, Nicole O, Docagne F, Sartelet H, Mackenzie ET, Vivien, D. (1998). Up-regulation of a serine protease inhibitor in astrocytes mediates the neuroprotective activity of transforming growth factor beta1. FASEB J 12:1683–1691.

Buisson A, Lesne S, Docagne F, Ali C, Nicole O, MacKenzie ET, Vivien, D. (2003). Transforming growth factor-beta and ischemic brain injury. Cell Mol Neurobiol 23:539–550.

Cook RH. (1979). Memory loss in Alzheimer disease. Ann Neurol 5: 105–106.

de Sampaio e Spohr TC, Martinez R, da Silva EF, Neto VM, Gomes FC. (2002). Neuro-glia interaction effects on GFAP gene: a novel role for transforming growth factor-beta1. Eur J Neurosci 16: 2059–2069.

Dhandapani KM, Hadman M, De Sevilla L, Wade MF, Mahesh VB, Brann DW. (2003). Astrocyte protection of neurons: Role of transforming growth factor-beta signaling via a c-Jun-AP-1 protective pathway. J Biol Chem 278:43329–43339.

Docagne F, Nicole O, Marti HH, MacKenzie ET, Buisson A, Vivien D. (1999). Transforming growth factor-beta1 as a regulator of the serpins/t-PA axis in cerebral ischemia. FASEB J 13:1315–1324.

Dorr AE, Lerch JP, Spring S, Kabani N, Henkelman RM. (2008). High resolution three-dimensional brain atlas using an average magnetic resonance image of 40 adult C57Bl/6J mice. Neuroimage 42:60–69.

Dupret D, Fabre A, Dobrossy MD, Panatier A, Rodriguez JJ, Lamarque S, Lemaire V, Oliet SH, Piazza PV, Abrous DN. (2007). Spatial learning depends on both the addition and removal of new hippocampal neurons. PLoS Biol 5, e214.

Eichenbaum H. (2004). Hippocampus: Cognitive processes and neural representations that underlie declarative memory. Neuron 44:109–120.

Genovese CR, Lazar NA, Nichols T. (2002). Thresholding of statistical maps in functional neuroimaging using the false discovery rate. Neuroimage 15:870–878.

Gundersen HJ, Jensen EB, Kieu K, Nielsen J. (1999). The efficiency of systematic sampling in stereology–reconsidered. J Microsc 193: 199–211.

Henrich-Noack P, Prehn JH, Krieglstein J. (1996). TGF-beta 1 protects hippocampal neurons against degeneration caused by transient global ischemia. Dose-response relationship and potential neuroprotective mechanisms. Stroke 27:1609–1614; discussion 1615.

Hensley K, Fedynyshyn J, Ferrell S, Floyd RA, Gordon B, Grammas P, Hamdheydari L, Mhatre M, Mou S, Pye QN, et al. (2003). Message and protein-level elevation of tumor necrosis factor alpha (TNF alpha) and TNF alpha-modulating cytokines in spinal cords of the G93A-SOD1 mouse model for amyotrophic lateral sclerosis. Neurobiol Dis 14:74–80.

Hosseini-Sharifabad M, Nyengaard JR. (2007). Design-based estimation of neuronal number and individual neuronal volume in the rat hippocampus. J Neurosci Methods 162:206–214.

Inokuchi K. (2011). Adult neurogenesis and modulation of neural circuit function. Curr Opin Neurobiol 21:360–364.

Kee N, Sivalingam S, Boonstra R, Wojtowicz JM. (2002). The utility of Ki-67 and BrdU as proliferative markers of adult neurogenesis. J Neurosci Methods 115:97–105.

Kim WR, Park OH, Choi S, Choi SY, Park SK, Lee KJ, Rhyu IJ, Kim H, Lee YK, Kim HT, et al. (2009). The maintenance of specific aspects of neuronal function and behavior is dependent on programmed cell death of adult-generated neurons in the dentate gyrus. Eur J Neurosci 29:1408–1421.

Krieglstein K, Zheng F, Unsicker K, Alzheimer C. (2011). More than being protective: functional roles for TGF-beta/activin signaling pathways at central synapses. Trends Neurosci 34:421–429.

Lee JW, Kim WR, Sun W, Jung MW. (2012). Disruption of dentate gyrus blocks effect of visual input on spatial firing of CA1 neurons. J Neurosci 32:12999–13003.

Lerch JP, Sled JG, Henkelman RM. (2011). MRI phenotyping of genetically altered mice. Meth Mol Biol 711:349–361.

Lindholm D, Castren E, Kiefer R, Zafra F, Thoenen H. (1992). Transforming growth factor-beta 1 in the rat brain: Increase after injury and inhibition of astrocyte proliferation. J Cell Biol 117: 395–400.

Link J, Soderstrom M, Olsson T, Hojeberg B, Ljungdahl A, Link H. (1994). Increased transforming growth factor-beta, interleukin-4, and interferon-gamma in multiple sclerosis. Ann Neurol 36:379–386.

Massague J. (2012). TGFbeta signalling in context. Nat Rev Mol Cell Biol 13:616–630.

Meltzer LA, Yabaluri R, Deisseroth K. (2005). A role for circuit homeostasis in adult neurogenesis. Trends Neurosci 28:653–660.

Mogi M, Harada M, Kondo T, Riederer P, Inagaki H, Minami M, Nagatsu T. (1994). Interleukin-1 beta, interleukin-6, epidermal growth factor and transforming growth factor-alpha are elevated in the brain from parkinsonian patients. Neurosci Lett 180:147–150.

Mogi M, Harada M, Kondo T, Narabayashi H, Riederer P, Nagatsu T. (1995). Transforming growth factor-beta 1 levels are elevated in the striatum and in ventricular cerebrospinal fluid in Parkinson's disease. Neurosci Lett 193:129–132.

Nichols NR, Finch CE. (1991). Transforming growth factor-beta1 mRNA decreases in brain in response to glucocorticoid treatment of adrenalectomized rats. Mol Cell Neurosci 2:221–227.

Nunez G, del Peso L. (1998). Linking extracellular survival signals and the apoptotic machinery. Curr Opin Neurobiol 8:613–618.

Pratt BM, McPherson JM. (1997). TGF-beta in the central nervous system: potential roles in ischemic injury and neurodegenerative diseases. Cytokine Growth Factor Rev 8:267–292.

Reilly JF, Maher PA, Kumari VG. (1998). Regulation of astrocyte GFAP expression by TGF-beta1 and FGF-2. Glia 22: 202–210.

Ruocco A, Nicole O, Docagne F, Ali C, Chazalviel L, Komesli S, Yablonsky F, Roussel S, MacKenzie ET, Vivien D, et al. (1999). A transforming growth factor-beta antagonist unmasks the neuroprotective role of this endogenous cytokine in excitotoxic and ischemic brain injury. J Cereb Blood Flow Metab 19: 1345–1353.

Sousa Vde O, Romao L, Neto VM, Gomes FC. (2004). Glial fibrillary acidic protein gene promoter is differently modulated by transforming growth factor-beta 1 in astrocytes from distinct brain regions. Eur J Neurosci 19:1721–1730.

Teixeira CM, Pomedli SR, Maei HR, Kee N, Frankland PW. (2006). Involvement of the anterior cingulate cortex in the expression of remote spatial memory. J Neurosci 26:7555–7564.

Tesseur I, Wyss-Coray T. (2006). A role for TGF-beta signaling in neurodegeneration: Evidence from genetically engineered models. Curr Alzheimer Res 3 505–513.

Treves A, Rolls, ET. (1994). Computational analysis of the role of the hippocampus in memory. Hippocampus 4:374–391.

Treves A, Tashiro A, Witter MP, Moser EI. (2008). What is the mammalian dentate gyrus good for? Neuroscience 154: 1155–1172.

van der Worp HB, Claus SP, Bar PR, Ramos LM, Algra A, van Gijn J, Kappelle LJ. (2001). Reproducibility of measurements of cerebral infarct volume on CT scans. Stroke 32:424–430.

West MJ, Coleman PD, Flood DG, Troncoso JC. (1994). Differences in the pattern of hippocampal neuronal loss in normal ageing and Alzheimer's disease. Lancet 344:769–772.

West MJ, Kawas CH, Stewart WF, Rudow GL, Troncoso JC. (2004). Hippocampal neurons in pre-clinical Alzheimer's disease. Neurobiol Aging 25:1205–1212.

Wyss-Coray T, Feng L, Masliah E, Ruppe MD, Lee HS, Toggas SM, Rockenstein EM, Mucke L. (1995). Increased central nervous system production of extracellular matrix components and development of hydrocephalus in transgenic mice overexpressing transforming growth factor-beta 1. Am J Pathol 147:53–67.

Wyss-Coray T, Masliah E, Mallory M, McConlogue L, Johnson-Wood K, Lin C, Mucke, L. (1997). Amyloidogenic role of cytokine TGF-beta1 in transgenic mice and in Alzheimer's disease. Nature 389:603–606.

Zetterberg H, Andreasen N, Blennow, K. (2004). Increased cerebrospinal fluid levels of transforming growth factor-beta1 in Alzheimer's disease. Neurosci Lett 367:194–196.

Zhao C, Deng W, Gage FH. (2008). Mechanisms and functional implications of adult neurogenesis. Cell 132:645–660.

Zhu Y, Ahlemeyer B, Bauerbach E, Krieglstein J. (2001). TGF-beta1 inhibits caspase-3 activation and neuronal apoptosis in rat hippocampal cultures. Neurochem Int 38:227–235.

Zhu Y, Yang GY, Ahlemeyer B, Pang L, Che XM, Culmsee C, Klumpp S, Krieglstein J. (2002). Transforming growth factor-beta 1 increases bad phosphorylation and protects neurons against damage. J Neurosci 22:3898–3909.